Macromolecules

ARTICLE

pubs.acs.org/Macromolecules

Thermal Elimination of Precursors to Poly(phenylenevinylene) with a Macrocounterion versus a Small Counterion: A Coordinated Experimental and Simulation Study

Lara A. Al-Hariri, Lianqing Zheng, Wei Yang, and Joseph B. Schlenoff*

Department of Chemistry and Biochemistry, Florida State University, Tallahassee, Florida 32306, United States

Supporting Information

ABSTRACT: Coordinated experimental and orthogonal space random walk (OSRW) molecular dynamics simulation studies were performed to understand the exceptionally low temperature required for thermal conversion of a poly(phenylenevinylene) (PPV) precursor containing the macromolecular counterion poly(ethylene glycol)-4-nonylphenyl-3-sulfopropyl ether (PEGNOPS). Simulations of this solvent-free system converged for starting points where the backbone was artificially expanded or compressed. In this example of a polymer organized by a polymer, the simulations revealed the ability of PEGNOPS to partially preorder the precursor chain in a conformation that favors the E2 elimination pathway.

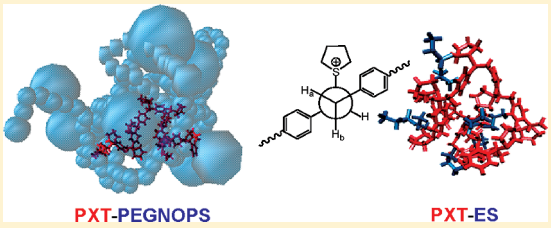

INTRODUCTION

Poly(phenylenevinylene) (PPV) and its derivatives are intensively studied conjugated polymers.[1] In addition to conductivity in the doped state, good thermal stability[2,3] and tunable luminescence in the undoped state have stimulated application of PPVs in (opto)electronic[4] devices such as organic light-emitting diodes (OLEDs),[3,5−7] field effect transistors,[3−5] photovoltaic cells,[3,5,6] and polymer lasers.[5,6] To prepare thin films, modification of the PPV backbone with hydrocarbon pendant groups yields soluble derivatives.[8,9] Alternatively, films may be cast from a high molecular weight water-soluble precursor, which is subsequently converted into the final polymer by thermal elimination (Scheme 1).

The optical and electrical properties of PPVs prepared by the thermal elimination route depend on many variables such as processing,[7] temperature of elimination,[1,10] compensating counterion,[11−13] and side chains in the precursor.[14] Such factors control the spatial orientation and intermolecular distance between conjugated segments,[15] the effective conjugation length,[2,10,15−17] and the extent of order of the backbone (crystallinity).[18,19]

Optical properties of PPV are understood and tuned through interactions of PPV segments. These interactions, leading to the formation of excimers, exiplexes, and aggregates that form a new ground state, were shown to decrease photoluminescence, PL. They are enhanced if PPV segments are in proximity. Yan et al.[20] indicated that amorphous PPV, in which chromophores are separated, have more efficient PL than crystalline PPV, where interchain fluorescence quenching takes place. Since then, there have been various attempts to promote separation between PPV chromophores. Kas et al.[15] enhanced PL by controlling the distance between conjugated segments of the PPV backbone and controlling orientation by grafting PPV as a side chain on a self-assembled α-helical peptide. Another commonly used method is the dilution of PPV segments by another nonconjugated polymer.[21] Son et al.[18] interrupted the conjugation of PPV by engineering cis linkages into the backbone, giving amorphous PPV that suppresses polymer packing and increases PL. Many groups have studied the effect of the length, flexibility, structure, and bulkiness of the side chain on the packing of PPV and consequent effects on the PL.[22−25]

For the aqueous elimination route (Scheme 1), an additional strategy for enhancing the PL efficiency has been to lower the temperature of elimination, which decreases the formation of quenching sites in the backbone of PPV. Convenient variables for modulating the temperature of elimination are choice of the counterion or leaving group (Scheme 1).[1] It was shown that tetrahydrothiophene (THT) gives a higher effective conjugation length at a lower temperature of elimination than dimethyl sulfide as a leaving group.[26] Marletta et al.[11] reported that poly(xylylidenetetrahydrothiophenium), PXT, films with dodecylbenzenesulfonate (DBS) as a counterion can be efficiently eliminated at 115 °C. In contrast, PPV films processed from PXT using chloride as counterion are prepared at 210 °C or more. This difference in processing temperatures was attributed to the relative stabilities of the sulfonium ion in the presence of different counterions.[11] The sulfonium group is believed to be more thermally stable when balanced with the anion of a stronger acid,[27] so a halide would be more stable than a sulfonate group, the former being less basic. However, in an earlier work, Beerden et al.[28] showed that elimination of PXT with a nucleophilic anion such as a halide required higher temperatures to eliminate a side product of the

Received: April 22, 2011
Revised: July 19, 2011
Published: August 03, 2011

ACS Publications © 2011 American Chemical Society

Scheme 1. (upper) Elimination of Poly(xylylidenetetrahydrothiophenium) Salts, PXT, and (lower) Structures of PEGNOPS ($n \sim 20$) and Ethanesulfonate, ES, Counterions[a]

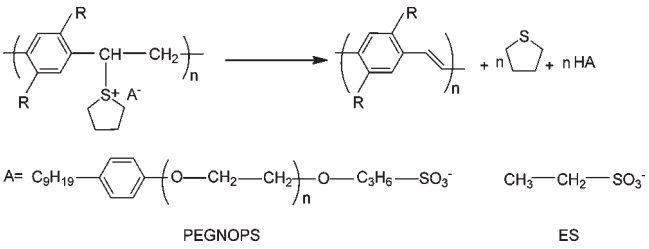

[a] In unsubstituted PXT, as used here, −R = −H.

reaction, which was a result of nucleophilic replacement of tetrahydrothiophene. In the present study, the use of a non-nucleophilic functional group (aliphatic sulfonate), whether as a small or a large anion, is essential to avoiding such possible side reactions.

Counterions employed in the aqueous routes of PPV have generally been small, such as Cl^-, CH_3COO^-, F^-, and Br^-.[12,28] The only two long-chain counterions used have been DBS[11] and perfluorononoate.[29] In spite of the variety of counterion sizes, the emphasis in past work for explaining elimination temperatures has been on the basicity of the counterion. Poly(styrenesulfonate) has been used as a polymeric counterion for PXT.[30,31] Abe et al.[32] reported that using polymers or polyelectrolytes as additives to the conjugated polyelectrolytes increased the PL by inducing order to the conjugated polyelectrolyte.

In a recent paper we reported that using poly(ethylene glycol)-4-nonylphenyl-3-sulfopropyl ether (PEGNOPS) as the counterion for PXT enhanced the PL due to the sacrificial and separation role that PEGNOPS played in suppressing carbonyl formation in the PPV backbone and interchain quenching, respectively. The fact that the elimination temperature was only 80 °C was difficult to explain, but it permitted elimination under ambient conditions. The use of long-chain counterions brings an interesting dimension into polyelectrolytes such as PXT: the morphology is essentially a bottlebrush, where the length of the side chains is varied simply by changing the counterion. If the chain length of the counterion is long enough, the environment of the backbone is then controlled by the counterion. In an effort to understand the role of this macrocounterion in PXT elimination, we performed complementary orthogonal space random walk (OSRW) molecular dynamics simulations, which suggested that the backbone conformation of PXT is favorably influenced by the ethylene oxide tails of the macrocounterion. To separate effects between those caused by headgroup chemistry and by the environment, we coordinated experiments and theory using a short-chain aliphatic sulfonate, which mimics the hydrophilic sulfonate end of PEGNOPS.

MATERIALS AND EXPERIMENTS

Ethanesulfonic acid, sodium salt form (ES), poly(ethylene glycol)-4-nonylphenyl-3-sulfopropyl ether potassium (PEGNOPS), and α,α′-dichloro-*p*-xylene (98%) were used as obtained from Aldrich. Poly(xylylidenetetrahydrothiophenium chloride) (PXT-Cl) was prepared from *p*-xylylenebis(tetrahydrothiophenium chloride) using a literature procedure.[33] PXT-Cl was purified by dialysis against distilled water using 12 000−14 000 molecular weight cutoff (MWCO) Spectra/Pro dialysis tubing.

PXT-ES preparation by ion exchange: PXT-Cl was dialyzed against a 0.1 M solution of ES for 1 day and then for 48 h against distilled water with a change of water each 8 h. PXT-PEGNOPS: 10 mM PXT-Cl was mixed with 1.42 mM PEGNOPS dissolved in ethanol (to give a several-fold excess of PEGNOPS), then dialyzed against 0.2 M PEGNOPS, and then against water for 48 h with a change of water each 8 h. Elemental analysis of the ion-exchanged PXT-PEGNOPS (Atlantic Microlab): C 57.05%, H 7.87%, S 7.71%, Cl 0.65%, implying that 78% of the chloride was exchanged by PEGNOPS. Films were cast under atmospheric conditions at room temperature on relevant substrates. Films were thermally annealed under atmospheric conditions in a heater fitted with a thermocouple in direct contact with the substrate. The term "ambient" is used to denote processing under the lab environment, which was about 40% relative humidity at 73 ± 3 °F in standard atmosphere.

UV−vis data were obtained using a Varian Cary 100 UV/vis double-beam spectrometer. Samples were prepared on round sapphire slides. Photoluminescence was recorded on a Cary Eclipse fluorescence spectrometer. Samples were excited at different wavelengths, and emission was scanned to 800 nm.

Computational methods: A recently developed accelerated molecular dynamics simulation method, "the orthogonal space random walk (OSRW) algorithm", was employed.[34] OSRW simulations were performed in a customized CHARMM program. The two model systems consisted of 10 PXT units with 10 ES as counterions (190 atoms) or 10 PXT units with 10 PEGNOPS as counterions (1920 atoms). The initial structure of each model system was built using the CHARMM Internal Coordinate (IC) facility. Since simulations were done to mimic PXT-ES and PXT-PEGNOPS films that have no water (solvent), simulations were done with no solvent. For each model PXT-PEGNOPS and PXT-ES two initial structures were generated via a restraint-minimization procedure with a PXT chain R_g 7 Å (termed the "compact" initial condition) and 16 Å (termed the "extended" initial condition). Simulations started from the compact and extended initial conditions to confirm that the models were not stuck in local minima during simulations. Similar results, attained independent of initial simulation starting conformation, indicate the robustness of the method. More extensive details on the model system setup and details of the method used are provided in the Supporting Information.

The simulations were performed at 80 °C (temperature at which the experiments were carried out) using OSRW and canonical ensemble simulations. Langevin dynamics were employed as the thermostat to control temperature with a friction coefficient of 60 ps^{-1} acting on all the heavy atoms. The random forces were set corresponding to the target temperature of 80 °C. The time step was 1 fs.

In all the recursion simulations, the height of the Gaussian function h (as in eq 4 in the Supporting Information) was set to 0.1 kcal/mol; the widths of the Gaussian function, ω_1 and ω_2, were set to 0.01 and 4 kcal/mol, respectively. In the PXT-PEGNOPS OSRW simulations, the lower bound scaling parameter λ_0 was set to 0.2 due to the fact that its energy landscape is more rugged; in the short surfactant model OSRW simulations, the lower bound scaling parameter λ_0 was set to 0.6. In the metadynamics recursion, $F_m(\lambda, \partial U_0/\partial\lambda)$ (based on eq 5 in the Supporting Information) was updated every 10 time steps; in the scaling parameter space recursion, $f_m(\lambda)$, was updated every 100 time steps. Each of the production simulations was initiated when the radius of the gyration of the target polymer chain converged in the corresponding recursion simulation.

RESULTS AND DISCUSSION

Studies on the mechanism of elimination of PXT are controversial. Many mechanisms were suggested, including E1cB, E1, and E2, but none of them are fully consistent with the experimental results.[1,12,26,35−37] E1cB can be discounted because of the following: the unfavorable thermodynamics for formation

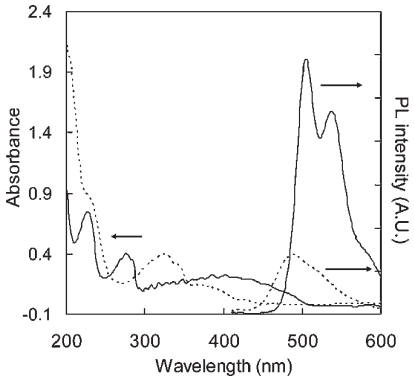

Figure 1. UV−vis and PL spectra excited at λ = 400 nm for PXT-PEGNOPS film thermally annealed at 80 °C in air for 20 min (solid spectra) and of PXT-ES film thermally annealed at 80 °C in air for 20 min (dotted spectra).

of the carbanion, lack of stabilizing groups and/or strong base, having THT which is a good leaving group and the fact that E1cB will yield a mixture of *cis*- and *trans*-PPV,[12,36] whereas reaction from the PXT route yields *trans*-PPV only.[18,38] Both Wang et al.[12] and Shah et al.[35] attempted to reconcile the controversy regarding the mechanism of elimination by suggesting that E2 occurs at low temperature (100−150 °C) while E1 is the dominant pathway at higher temperatures.

In the literature on elimination mechanisms, only the basicity of the counterion was considered, where most of the counterions used were small.[12] Although Marletta et al.[11] used (the larger) DBS and perfluorononoate counterions, they did not look into the effect of counterion chain length on elimination. If the final conjugated polymer is charged, its photophysical properties may be strongly influenced by the counterion. For example, Abe et al.[32] explored the effect of polyelectrolyte counterions on the PL of a charged PPV derivative. These authors showed that when polymers and/or polyelectrolytes were used as counterions, PL in the conjugated polyelectrolyte was strongly enhanced.[32] Polyelectrolytes as counterions provide approximately the same mass/charge ratio as do small organic ions. In contrast, PEGNOPS, charged only at one end, provides significantly more mass/charge. The elimination occurs at 80 °C, a temperature region where the E2 mechanism dominates.

Figure 1 shows absorption and normalized PL spectra of PXT-ES and PXT-PEGNOPS thermally annealed films at 80 °C in air for 20 min under ambient conditions. PPV prepared from PXT-PEGNOPS has a broad UV−vis absorption spectrum due to the wide distribution of conjugation lengths. The absorbance peak centered at 410 nm and extending to 500 nm implies the presence of long conjugated segments in the backbone. On the other hand, material prepared from PXT-ES has a narrower absorbance band centered at 325 nm and a shoulder at 370 nm. This relatively narrow absorbance indicates that shorter conjugation lengths of PPV result from PXT-ES. Absorption is an instantaneous phenomenon during which no vibrational relaxation takes place, whereas PL originates from the most stable excited vibrational state following spectral diffusion which leads to better-resolved PL peaks.[39] The PL of PXT-PEGNOPS is 4 times higher in intensity and more red-shifted than PXT-ES. These significant differences are observed in spite of the fact that the charges on both counterions are aliphatic with the same basicity (same functional group).

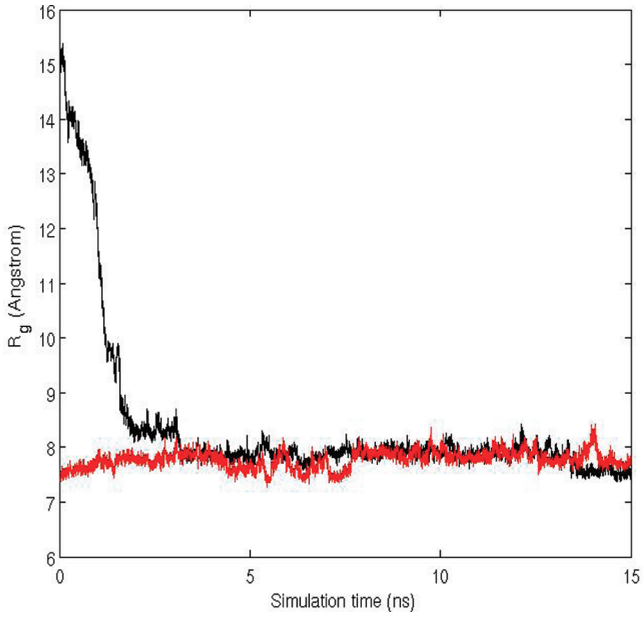

Figure 2. Radius of gyration evolution of 10 monomer units of PXT chain of PXT-ES vs time of OSRW simulation at 80 °C.

Traditionally, the wide absorption band with a maximum at about 400 nm, but extending up to about 500 nm, is used as an indication of the extent of conjugation.[40] However, it has been shown that this band is subject to other variables, such as the extent of exciton delocalization.[41] In addition, extent of delocalization may not correlate directly with extent of elimination if PPV with defects (e.g., cis linkages) is produced. The extent of elimination is more directly gauged from the decrease of the UV absorbance due to the PXT repeat unit, at 320 nm. In this respect, PXT-PEGNOPS clearly shows more extensive elimination than the PXT-ES (Figure 1).

To gain insight into the reasons for the low temperature elimination, OSRW molecular dynamics simulations[34] were carried out on both PXT-ES and PXT-PEGNOPS models. Both models consisted of 10 PXT units with 10 PEGNOPS/ES counterions assuming ion exchange is 100%. Figure 2 shows the time-dependent evolution of the radius of gyration of the PXT chain for the PXT-ES system starting from two different initial conditions. The convergence of two recursion simulations from two starting structures—the compact one with the radius of gyration of 7.8 Å and the extended one with the radius of gyration of 15 Å—demonstrates the sampling adequacy. In other words, it demonstrates that none of the models are trapped in local minima during simulation and that a global minimum is achieved. Note that only very slight initial compaction was possible, as the final structure is already a compact, random-coil, space-filling structure. Sampling adequacy is also demonstrated in the convergence of the PXT-PEGNOPS simulation in Figure 3. It is noteworthy that the recursion simulations on the PXT-PEGNOPS model converged after around 20 ns to the global minimum (R_g = 8.8 Å), whereas the PXT-ES model reached the global minimum (R_g = 7.8 Å) after 2.5 ns. This is due to the longer chain of PEGNOPS that takes more time to relax. The conformation of PXT-PEGNOPS and that of PXT-ES in their most stable conformations are represented in Scheme 2. It is clear from the equilibrium R_g values in Figures 2 and 3 that the PXT chain is slightly more expanded in PEGNOPS compared to ES.

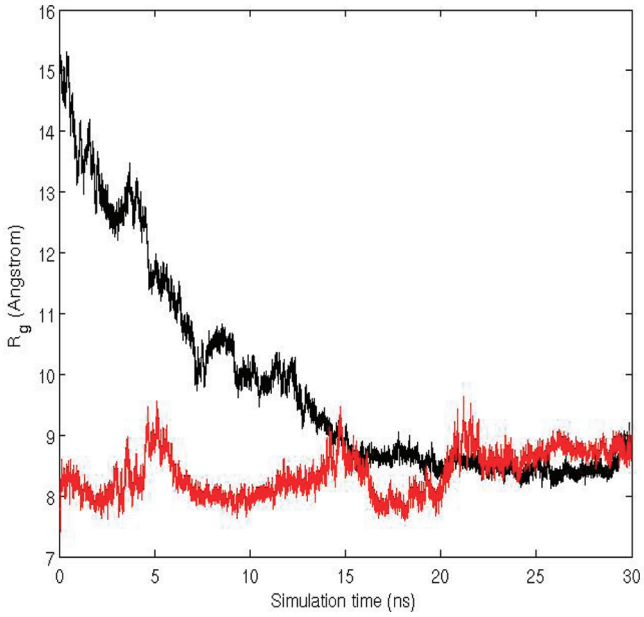

Figure 3. Radius of gyration evolution of 10 units of a PXT chain for PXT-PEGNOPS vs time. OSRW simulation done at 80 °C.

Scheme 2. Molecular Modeling of (a) PXT-PEGNOPS in Its Most Stable Conformation and (b) PXT-ES in Its Most Stable Conformation[a]

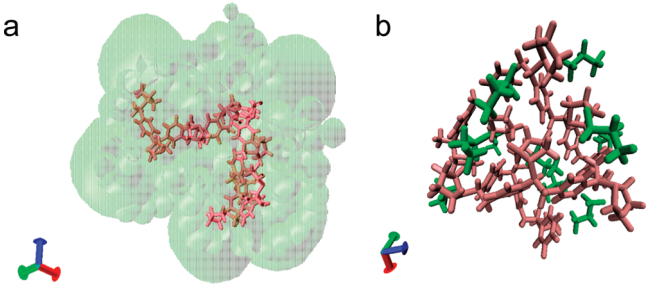

[a] PXT main chain is brick red, and the molecules in green are the counterions.

The much larger volume occupied by PEGNOPS, which causes this chain expansion, is clearly seen in Scheme 2. The environment for the polyelectrolyte is controlled by its PEGNOPS counterion.

Figures 4 and 5 respectively reveal the free energy surfaces of the PXT-ES and PXT-PEGNOPS models in the space described by the C−C/C−S dihedral angle (shown in Scheme 3) and the radius of gyration of PXT. The C−C/C−S dihedral angle describes the relative orientation between the THT and the benzene ring as shown in Scheme 3.

For PXT-ES the most populated conformational regions are those with C−C/C−S dihedral angles around 0−20°, 50−85°, and 140−180° (Figure 4). In comparison, for PXT-PEGNOPS the conformational region with C−C/C−S dihedral angles from 20° to 180° are well populated (Figure 5). It is well-known that for E2 elimination the leaving group, THT, and one of the hydrogen atoms (Scheme 3, H_a and H_b) should be in the anti positions; i.e., the H−C/C−S dihedral angle between the two should be around 180° (Scheme 3). Table 1 illustrates examples of the H−C/C−S dihedral angles at which the E2 mechanism is

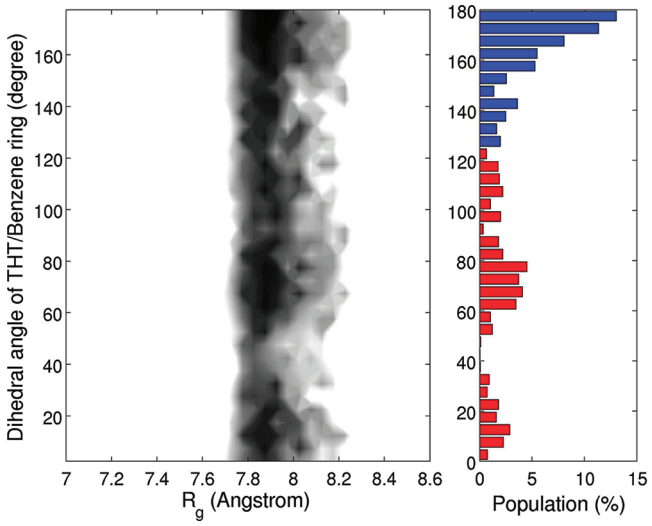

Figure 4. Potential of free energy surface of PXT-ES at 80 °C vs R_g. Column on the right shows dihedral angle vs % of population. The red zone in % of population represents the reactive region for trans elimination, and the blue zone represents the nonreactive region for trans elimination.

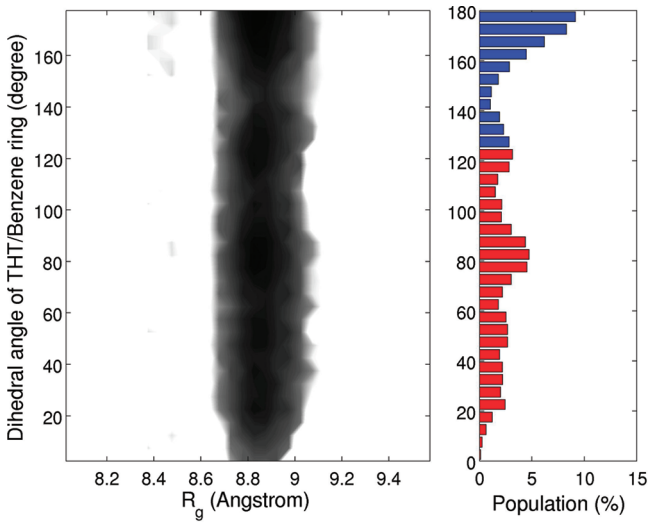

Figure 5. Potential of free energy surface of PXT-PEGNOPS at 80 °C vs R_g. Column on the right shows dihedral angle vs % of population. The red zone in % population represents the active region for trans elimination, and the blue zone represent the nonreactive region for trans elimination.

Scheme 3[a]

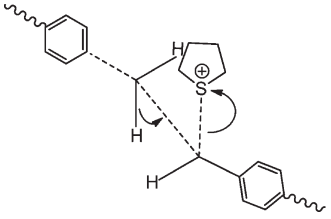

[a] The dashed lines are the C−C/C−S dihedral angle optimized for the E2 elimination mechanism shown by the arrows.

Table 1. PXT Conformations for Different Dihedral Angles and E2 Mechanism Reactivity at That Angle[a]

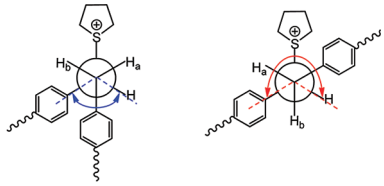

THT/Benzene dihedral angle	180 °	60 °
THT/ H_b dihedral angle	60 °	180 °
	Non reactive region	Reactive region

[a] On the left, the front benzene within the range of conformations shown by the blue arrow places the system in the "nonreactive" conformation shown in Figures 4 and 5. On the right, the front benzene within the angle subtended by the red arrow represents the "reactive" zone, where H_a or H_b is within 60° of the optimum conformation for E2 elimination.

Scheme 4. Molecular Modeling of PEGNOPS in the Film Showing Bundles Formed by PEG Units

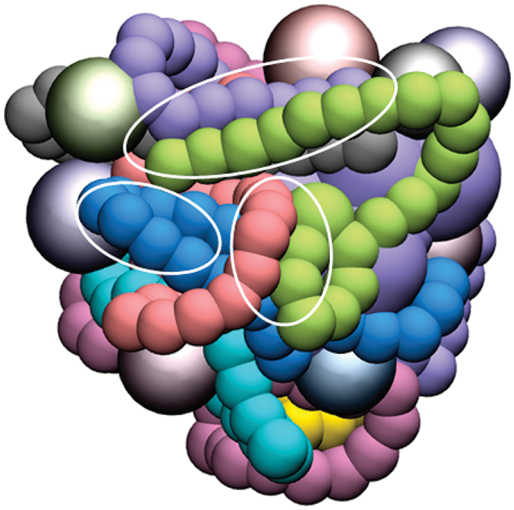

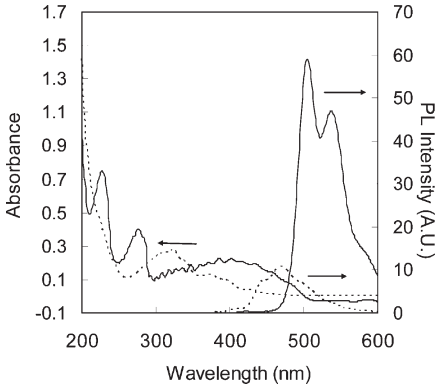

Figure 6. UV−vis and PL spectra of PXT−PEGNOPS film thermally annealed at 80 °C in air for 20 min (solid line) and of PXT-PEGNOPS solution thermally annealed at 80 °C for 120 min (dotted line). The PXT-PEGNOPS solution was at a concentration of about 0.8 mM.

possible, where the THT group and one of the hydrogens (H_a, H_b) is in the anti position. The C−S/C−C dihedral angles between 0° and 120° encompass the reactive region (Figures 4 and 5, red zone in % population), where the E2 reaction is promoted. The region between 120° and 180° is the nonreactive region (Figure 4 and 5, blue zones in % population)

In the PXT-ES model 42% of the population is in the reactive region (0−120°), whereas for the PXT-PEGNOPS complex the percentage is 55%. Thus, the reactive region in PXT-PEGNOPS is about 30% more populated than that of PXT-ES; i.e., there is about 30% more chance to have the hydrogen atom located in the anti position in PXT-PEGNOPS than in PXT-ES. This result is consistent with the experiments that showed that PPV produced from PXT-PEGNOPS has higher conjugation length than PPV from PXT-ES (Figure 1, UV−vis) although both of them are processed under the same conditions.

It appears that the 20 PEG units in the backbone of PEG-NOPS form bundles around the PXT chain due to intra- and intermolecular hydrogen bonding between PEG units (Scheme 4 and Scheme S1). Such H-bonding is possible in the absence of water. The bundles organize the PXT chain in a conformation that favors E2 elimination.

To support the idea that PXT needs to be organized in the solid state, Figure 6 compares UV−vis spectra of PXT-PEG-NOPS thermally eliminated in solution versus in film at the same temperature (80 °C). PPV-PEGNOPS prepared in film form is more red-shifted in both absorption and emission spectra. The shorter fluorescence wavelength of PXT-PEGNOPS in solution is due to the shorter length of conjugation of PPV. In solution, PEG hydrogen bonds with water whereas in the PXT-PEG-NOPS film PEG has the opportunity to H-bond with itself. The vibronic peaks in the fluorescence spectrum of PXT-PEGNOPS in the film are well developed and overlap with the fluorescence peak from shorter conjugated length PPV segments.[42] As in Figure 1, the relative decrease of the PXT absorption band at about 320 nm in Figure 6 is a relative measure of the extent of elimination of the PXT in the two very different environments. It is clear that the aqueous system eliminates incompletely at 80 °C. In addition, fully eliminated PPV is insoluble in all solvents.[43,44] The fact that it remained in solution shows it was less than about 50% eliminated.[12] Thus, the results of Figure 6 are consistent with the thesis that PEG units in PEGNOPS play a role in preordering the PXT chain prior to elimination when the system is in the solid state.

■ CONCLUSIONS

The counterion has proven to be a convenient and versatile variable for controlling the solution properties of conjugated

polymers. In the solid state, the PEGNOPS aliphatic sulfonate used here occupies most of the volume of the PXT precursor chain. The environment for thermal elimination of PXT films is now defined by the counterion, and PXT chain segments are well isolated. The molecular dynamics computational study revealed partial control of the PXT backbone configuration by the polyether tails of the PEGNOPS, setting up the molecule for elimination in the preferred trans geometry at 80 °C, the lowest temperature reported for efficient elimination of PXT to yield photoluminescing PPV.

■ ASSOCIATED CONTENT

Ⓢ Supporting Information. FT-IR spectra of PXT-PEG-NOPS film and PEGNOPS in solution and details of computation method. This material is available free of charge via the Internet at http://pubs.acs.org.

■ AUTHOR INFORMATION

Corresponding Author
*Tel (850) 644-3001; fax (850) 644-8281, e-mail schlen@chem.fsu.edu.

■ ACKNOWLEDGMENT

This work was supported by grants from the National Science Foundation (DMR 0309441 and MCB0919983).

■ REFERENCES

(1) De Kok, M. M.; Van Breemen, A. J. J. M.; Carleer, R. A. A.; Adriaensens, P. J.; Gelan, J. M.; Vanderzande, D. J. *Acta Polym.* **1999**, *50*, 28–34.
(2) Grage, M. M. L.; Wood, P. W.; Ruseckas, A.; Pullerits, T.; Mitchell, W.; Burn, P. L.; Samuel, I. D. W.; Sundstrom, V. *J. Chem. Phys.* **2003**, *118*, 7644–7650.
(3) Yousaf, S. M.; Bower, K. E.; Sychov, M. M.; Yousaf, M. R. *J. Mater. Sci.* **2005**, *40*, 5507–5510.
(4) Chen, L.-M.; Hong, Z.; Li, G.; Yang, Y. *Adv. Mater.* **2009**, *21*, 1434–1449.
(5) Feast, W. J.; Cacialli, F.; Koch, A. T. H.; Daik, R.; Lartigau, C.; Friend, R. H.; Beljonne, D.; Bredas, J.-L. *J. Mater. Chem.* **2007**, *17*, 907–912.
(6) Prelipceanu, M.; Prelipceanu, O.-S.; Tudose, O.-G.; Leontie, L.; Grimm, B.; Schrader, S. *Mater. Sci. Semicond. Process* **2007**, *10*, 77–89.
(7) Grimsdale, A. C.; Leok Chan, K.; Martin, R. E.; Jokisz, P. G.; Holmes, A. B. *Chem. Rev.* **2009**, *109*, 897–1091.
(8) Webster, G. R.; Whitelegg, S. A.; Bradley, D. D. C.; Burn, P. L. *Synth. Met.* **2001**, *119*, 269–270.
(9) Schoo, H. F. M.; Demandt, R. J. C. E. *Philips J. Res.* **1998**, *51*, 527–533.
(10) Papadimitrakopoulos, F.; Konstadinidis, K.; Miller, T. M.; Opila, R.; Chandross, E. A.; Galvin, M. E. *Chem. Mater.* **1994**, *6*, 1563–8.
(11) Marletta, A.; Gonçalves, D.; Oliveira, O. N., Jr.; Faria, R. M.; Guimarães, F. E. *Adv. Mater.* **2000**, *12*, 69–74.
(12) Schlenoff, J. B.; Wang, L. J. *Macromolecules* **1991**, *24*, 6653–9.
(13) Marletta, A.; Castro, F. A.; Borges, C. A. M.; Oliveira, O. N., Jr.; Faria, R. M.; Guimarães, F. E. G. *Macromolecules* **2002**, *35*, 9105–9109.
(14) Kesters, E.; de Kok, M. M.; Carleer, R. A. A.; Czech, J. H. P. B.; Adriaensens, P. J.; Gelan, J. M.; Vanderzande, D. J. *Polymer* **2002**, *43*, 5749–5755.
(15) Kas, O. Y.; Charati, M. B.; Rothberg, L. J.; Galvin, M. E.; Kiick, K. L. *J. Mater. Chem.* **2008**, *18*, 3847–3854.
(16) Moses, D.; Schmechel, R.; Heeger, A. J. *Synth. Met.* **2003**, *139*, 807–810.
(17) Yaliraki, S. N.; Silbey, R. J. *J. Chem. Phys.* **1996**, *104*, 1245–53.
(18) Son, S.; Dodabalapur, A.; Lovinger, A. J.; Galvin, M. E. *Science* **1995**, *269*, 376–8.
(19) Nelson, J.; Kwiatkowski, J. J.; Kirkpatrick, J.; Frost, J. M. *Acc. Chem. Res.* **2009**, *42*, 1768–1778.
(20) Yan, M.; Rothberg, L.; Galvin, M. E.; Miller, T. M.; Papadimitrakopoulos, F. *Int. SAMPE Tech. Conf.* **1995**, *27*, 694–702.
(21) Cheng, H.-L.; Lin, K.-F. *J. Polym. Res.* **1999**, *6*, 123–131.
(22) Kimura, M.; Sato, M.; Adachi, N.; Fukawa, T.; Kanbe, E.; Shirai, H. *Chem. Mater.* **2007**, *19*, 2809–2815.
(23) Schwartz, B. J. *Annu. Rev. Phys. Chem.* **2003**, *54*, 141–172.
(24) Peng, K.-Y.; Chen, S.-A.; Fann, W.-S.; Chen, S.-H.; Su, A.-C. *J. Phys. Chem. B* **2005**, *109*, 9368–73.
(25) Winokur, M. J.; Chunwachirasiri, W. *J. Polym. Sci., Part B: Polym. Phys.* **2003**, *41*, 2630–2648.
(26) Shah, H. V.; McGhie, A. R.; Arbuckle, G. A. *Thermochim. Acta* **1996**, *287*, 319–326.
(27) Era, M.; Kamiyama, K.; Yoshiura, K.; Momii, T.; Murata, H.; Tokito, S.; Tsutsui, T.; Saito, S. *Thin Solid Films* **1989**, *179*, 1–8.
(28) Beerden, A.; Vanderzande, D.; Gelan, J. *Synth. Met.* **1992**, *52*, 387–94.
(29) Wu, A.; Yokoyama, S.; Watanabe, S.; Kakimoto, M.-a.; Imai, Y.; Araki, T.; Iriyama, K. *Thin Solid Films* **1994**, *244*, 750–3.
(30) Fou, A. C.; Onitsuka, O.; Ferreira, M.; Rubner, M. F.; Hsieh, B. R. *J. Appl. Phys.* **1996**, *79*, 7501–7509.
(31) Tarabia, M.; Hong, H.; Davidov, D.; Kirstein, S.; Steitz, R.; Neumann, R.; Avny, Y. *J. Appl. Phys.* **1998**, *83*, 725–732.
(32) Abe, S.; Chen, L. *J. Polym. Sci., Part B: Polym. Phys.* **2003**, *41*, 1676–1679.
(33) Wessling, R. A.; Zimmerman, R. G. Polyelectrolytes from bis sulfonium salts. U.S. Patent 591706, Nov 1968.
(34) Zheng, L.; Chen, M.; Yang, W. *Proc. Natl. Acad. Sci. U. S. A.* **2008**, *105*, 20227–20232.
(35) Shah, H. V.; Arbuckle, G. A. *Macromolecules* **1999**, *32*, 1413–1423.
(36) Garay, R. O.; Sarimbalis, M. N.; Hernandez, S. A.; Montani, R. S. *Macromolecules* **2000**, *33*, 4398–4402.
(37) Cho, B. R. *Prog. Polym. Sci.* **2002**, *27*, 307–355.
(38) Kesters, E.; Gillissen, S.; Motmans, F.; Lutsen, L.; Vanderzande, D. *Macromolecules* **2002**, *35*, 7902–7910.
(39) Pichler, K.; Halliday, D. A.; Bradley, D. D. C.; Burn, P. L.; Friend, R. H.; Holmes, A. B. *J. Phys.: Condens. Matter* **1993**, *5*, 7155–72.
(40) Herold, M.; Gmeiner, J.; Riess, W.; Schwoerer, M. *Synth. Met.* **1996**, *76*, 109–12.
(41) Yan, M.; Rothberg, L. J.; Kwock, E. W.; Miller, T. M. *Phys. Rev. Lett.* **1995**, *75*, 1992–5.
(42) Rauscher, U.; Schütz, L.; Greiner, A.; Bässler, H. *J. Phys.: Condens. Matter* **1989**, *1*, 9751–63.
(43) Chaieb, A.; Vignau, L.; Brown, R.; Wantz, G.; Huby, N.; Francois, J.; Dagron-Lartigau, C. *Opt. Mater.* **2008**, *31*, 68–74.
(44) Wong, J. E.; Detert, H.; Brehmer, L.; Schrader, S. *Appl. Surf. Sci.* **2005**, *246*, 458–463.